Nuclear Engineering and Design 267 (2014) 23–33

Contents lists available at ScienceDirect

Nuclear Engineering and Design

journal homepage: www.elsevier.com/locate/nucengdes

Pre-conceptual core design of SCWR with annular fuel rods

Chuanqi Zhao[a,b], Liangzhi Cao[a,b,*], Hongchun Wu[b], Youqi Zheng[b]

[a] Key Laboratory of Thermo-Fluid Science and Engineering of MOE, School of Energy and Power Engineering, Xi'an Jiaotong University, Xi'an, Shaanxi 710049, China
[b] School of Nuclear Science and Technology, Xi'an Jiaotong University, Xi'an, Shaanxi 710049, China

HIGHLIGHTS

- Annular fuel with both internal and external cooling is used in supercritical light water reactor (SCWR).
- The geometry of the annular fuel has been optimized to achieve better performance for the SCWR.
- Based on the annular fuel assembly, an equilibrium core has been designed.
- The results show that the equilibrium core has satisfied all the objectives and design criteria.

ARTICLE INFO

Article history:
Received 13 July 2013
Received in revised form 30 October 2013
Accepted 2 November 2013

ABSTRACT

The new design of supercritical light water reactor was proposed using annular fuel assemblies. Annular fuel consists of several concentric rings. Feed water flows through the center and outside of the fuel to give both internal and external cooling. Thanks to this feature, the fuel center temperature and the cladding temperature can be reduced and high power density can be achieved. The water flowing through the center also provides moderation, so there is no need for extra water rods in the assembly. The power distribution can be easily flattened by use of this design. The geometry of the annular fuel has been optimized to achieve better performance for the SCWR. There are 19 fuel pins in an assembly. Burnable poison is utilized to reduce the initial excess reactivity. The fuel reloading pattern and water flow scheme were optimized to achieve more uniform power distribution and lower cladding temperature. An equilibrium core has been designed and analyzed using three dimensional neutronics and thermal-hydraulics coupling calculations. The void reactivity, Doppler coefficient and cold shut down margin were calculated for safety consideration. The present results show that this concept is a promising design for the SCWR.

1. Introduction

Supercritical light water reactor (SCWR) is a reactor cooled and moderated by supercritical water. It can be designed as thermal or fast reactor. Water does not exhibit a phase change from liquid to gas above 22.1 MPa. Therefore, the plant system is simpler and more compact than PWRs and BWRs without a dryer, water-steam separators and recirculation pumps. The coolant outlet temperature is high because there is no limitation of saturation temperature at supercritical pressure. This results in high thermal efficiency, which is good not only for producing electricity but also for reducing the amount of spent fuel per generated watt of electricity.

In the past years, extensive research and development (R&D) activities have been carried out covering various aspects of the SCWR development. The High Temperature Supercritical-Pressure Light Water Reactor (SCLWR-H) and the Super Light Water Reactor (Super LWR) have been proposed in Japan (Yamaji et al., 2005a,b; Kamei et al., 2006). In these designs, the square arranged fuel assembly with single row of fuel rods between water rods is used. The water rods improve neutron moderation. However, they cause heterogeneous moderation. The square fuel assembly has also been used in the High Performance Light Water Reactor (HPLWR) (Schulenberg et al., 2011; Maráczy et al., 2011). In this assembly, there is one water rod in the center surrounded by two rows of fuel rods. Fuel rods with lower enrichment are placed in the corner of the fuel assembly to overcome the heterogeneous moderation. Another solution for moderation problem is the double-row-rod assembly (Liu and Cheng, 2010; Zhao et al., 2013). It is also a square assembly with water rods and there are two rows of fuel rods between water rods. This assembly achieves more uniform moderation than the one-row-rod assembly (Liu and Cheng, 2009). The heterogeneous moderation still exists.

Annular fuels have been proposed and developed at MIT (Feng, 2006; Ellis, 2006; Paolo, 2005). The annular fuel has both internal

* Corresponding author at: School of Nuclear Science and Technology, Xi'an Jiaotong University, 28 Xianning West Road, Xi'an 710049, China. Tel.: +86 2982663285; fax: +86 2982668916.
E-mail addresses: caolz@mail.xjtu.edu.cn, caoliangzhi@gmail.com (L. Cao).

0029-5493/$ – see front matter © 2013 Elsevier B.V. All rights reserved.
http://dx.doi.org/10.1016/j.nucengdes.2013.11.070

and external cooling. Many researches have been done to optimize the geometrical parameters of an annular fuel assembly for both PWRs and BWRs to achieve maximum power. Feng (2006) showed that the best and optimum size of fuel rods that fits in the solid-cylindrical reference assembly dimension is a 13×13 array. With proportional increase in coolant flow rate, this annular fuel can increase PWR power density by 50% with the same DNBR margin, while reducing the peak fuel temperature by 1000 K. However if $UO_2$is used for the same cycle length, the assembly will be enriched higher (~8%). Ellis (2006) showed that a 5% enriched uranium nitride (UN) annular fuel assembly can operate at 150% power density for about 50 effective-full-power-days more than that of the nominal 17×17 ordinary solid-fuel-pin assembly which has being operating at 100% power density. Paolo (2005) had examined the potential for increasing the power density in BWRs using annular fuel. Different bundle designs were selected. It is found that the power density increase with annular fuel in BWRs may reach up to 23%. In the present studies, the annular fuel assembly was also used for SCWR design. Moderator flows through the center of the fuel. Thus the moderation is uniform for all fuel rods. This brings more uniform power distribution in an assembly. Because of both internal and external cooling, a high linear power density can be achieved while keeping the fuel temperature low. The high power density will lower the cost of nuclear energy. Using coupled model of three-dimensional neutronics and thermal-hydraulics, the Supercritical Water-cooled Reactor with Annular fuel rods (SCWR-A) was designed and analyzed.

This paper is organized as follows. Section 1 introduces the methods used in assembly and core design. Section 2 describes some optimizations for fuel assembly design. Section 3 illustrates some studies on the core design. Finally, some results and conclusions are summarized in Section 4 and Section 5.

2. Core design method

2.1. Neutronic calculations and coupling method

The flow chart of coupling calculation is shown in Fig. 1. The DRAGON code (Marleau et al., 2000) based on collision probability techniques was used to perform the two-dimensional assembly transport calculation for lattice physics study and to generate the macroscopic cross sections and diffusion coefficients for subsequent core calculations. Cross sections were taken from the 69-group WIMS-D library based on ENDF/B-VII data. Two-dimensional fuel assembly burnup calculations were carried out with expected water densities in the equilibrium core. At the end of burnup calculation, the energy groups were collapsed to four energy groups (2 fast and 2 thermal), and homogenized macroscopic cross sections were obtained for the fuel assembly as a function of water density and burnup.

Core depletion calculation was based on three-dimensional multi-group diffusion code CITATION (Fowler et al., 1971). As CITATION has no function of depletion calculation, an auxiliary code CTBurn has been developed (Yang et al., 2011). The calculation was carried out in one-sixth core symmetry using four energy groups, which correspond to the four collapsed energy groups obtained by the fuel assembly burnup calculations. In order to balance between the computational efficiency and accuracy, the mesh division is optimized as shown in Fig. 2. The radial mesh size is 3.5 cm for each equilateral triangle and the axial mesh size is 10.5 cm.

The dramatic change in water density makes neutronics and thermal-hydraulic coupling calculation necessary. The flowchart is shown in the red frame in Fig. 1. With designed core parameters and initial 3-D water density distribution for each calculation mesh, the core calculation is carried out. After this, a 3-D power distribution is obtained. Then the power distribution is used as input for thermal calculation to get a new water density distribution. The initial density distribution and the new one are compared. If not converged, the weighted average value of these two distributions is taken as new input for another core calculation. This procedure will continue until the water density distribution converges.

2.2. Thermal hydraulic calculations

The thermal-hydraulic parameters for the supercritical water are calculated with a Microsoft Excel Add-In (Spang, 2010) which is based on the industrial standard IAPWS-IF97. The code can calculate properties in the single-phase state for temperatures $273.15\ K < T < 1073.15\ K$ and pressures $0 < p < 100$ MPa. The thermal hydraulic calculations were carried out using in-house code Single-SC based on single-channel model. The single-channel model does not consider the pressure drops and only takes into account the

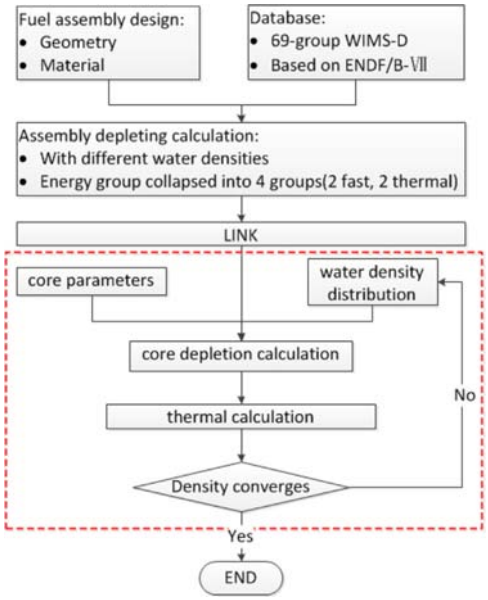

Fig. 1. Flow chart of coupling calculation.

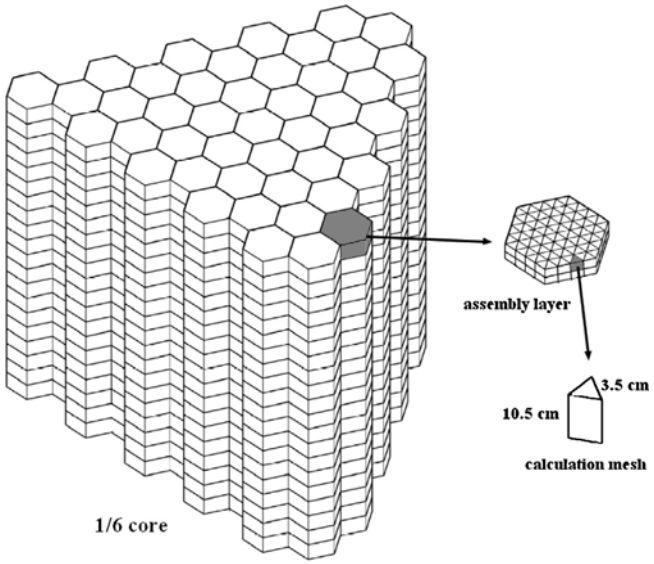

Fig. 2. 3D core geometry and mesh division.

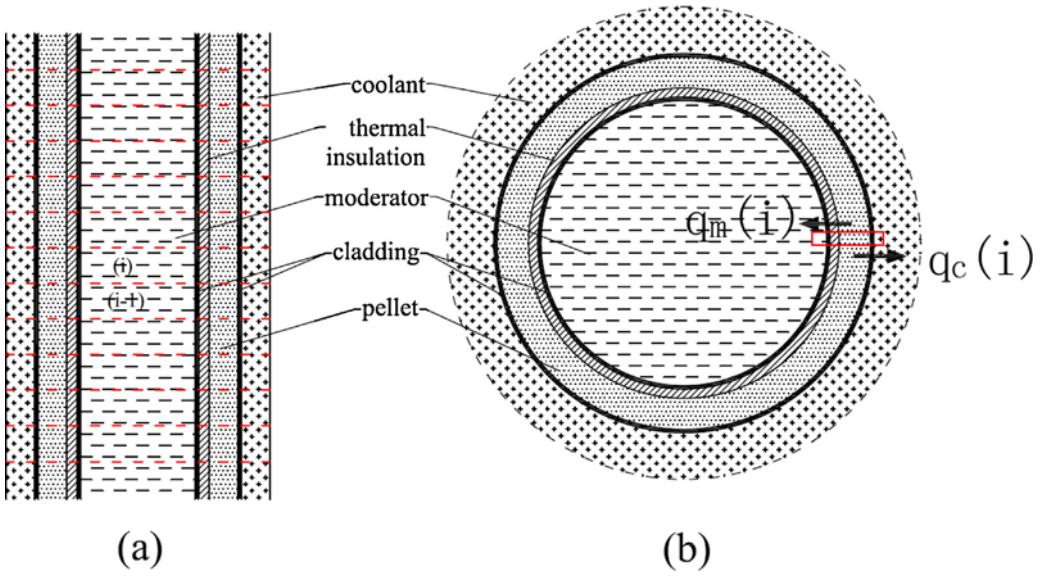

Fig. 3. Axial (a) and radial (b) view of single channel model.

conservations of energy and mass. In the calculation, each channel is divided into many meshes axially as shown in Fig. 3(a). The conservation of energy is expressed as follows:

$$q_x(i) = w_{x,i} \cdot H(P_{x,i}, T_{x,i}) - w_{x,i-1} \cdot H(P_{x,i-1}, T_{x,i-1}),$$
$$x = \text{coolant}, \quad \text{moderator}, \tag{1}$$

where $q_x(i)$ is the heat transferred to the coolant or moderator, H is the enthalpy, $w_{x,i}$ is the coolant or moderator flow rate at the (i)th mesh, $P_{x,i}$ and $T_{x,i}$ are the pressure and temperature at the (i)th mesh, respectively. The conservation of mass is expressed as follows:

$$w_x = w_{x,i} = w_{x,i-1} \tag{2}$$

After the axial heat transport calculation, the radial heat convection and conduction are carried out. The annular fuel is divided into many control volumes as shown in Fig. 3(b). The detail of the red frame in Fig. 3(b) is shown in Fig. 4. The note (m) and (c) stands for moderator and coolant, respectively. Control volume (1) and (n) is inner and outer cladding surface, respectively. For control volume (1), the conservation of energy is express as follows:

$$h_m \cdot 2\pi r_1 (T_m - T_1) + \lambda_{1,2} \cdot 2\pi \left(r_1 + \frac{D_{1,2}}{2}\right) \frac{T_2 - T_1}{D_{1,2}} = 0, \tag{4}$$

where h_m is the heat transfer coefficient of moderator, $r_i, i = 1, 2, \ldots, n$ is the radius of the center point of control volume (i), $T_i, i = m, 1, 2, \ldots, n, c$ is the temperature of control volume (i), $D_{i,i+1}, i = 1, 2, \ldots, n$ is the distance between of control volume (i) and $(i+1)$, $\lambda_{i,i+1}, i = 1, 2, \ldots, n$ is the average conduct coefficient of control volume (i) and $(i+1)$. The first term on the left is heat transferred from moderator to control volume (1). The second term on the left is heat conducted from control volume (2) to control volume (1).

Similar formula can be written for control volume (n) as follows:

$$\lambda_{n-1,n} \cdot 2\pi \left(r_n - \frac{D_{n-1,n}}{2}\right) \frac{T_{n-1} - T_n}{D_{n-1,n}} + h_c \cdot 2\pi r_n (T_c - T_n) = 0, \tag{5}$$

The first term on the left is heat conducted from volume $(n-1)$ to (n). The second term on the left is heat transferred from coolant to volume (n).

For control volume (j), the conservation of energy is express as follows:

$$q_{j-1,j} + Q_j = q_{j,j+1}, \tag{6}$$

where $q_{j-1,j}$ is the heat transferred from control volume $(j-1)$ to control volume (j), Q_j is the heat generated in control volume (j). For cladding or thermal insulation, Q_j equals to zero.

Each fuel assembly in the core was treated as one channel. Parallel calculation was introduced to save time. The single-channel calculation was carried out with two types of channels: the average channel was applied to calculate the coolant and moderator density distribution and the hot channel was applied to calculate the maximum cladding surface temperature (MCST) and maximum fuel temperature (MFT). Heat transfer coefficients were determined by the Watts correlation (Watts and Chou, 1982). With the spatial power distribution calculated by core depletion calculation, average and maximum power of each assembly can be obtained at all burnup steps. Considering maximum power of each assembly through the whole cycle, the core coolant flow rate distribution can be searched to satisfy the MCST limitation. With the flow rate distribution, water density distributions at all burnup steps can be calculated using average power of each assembly. The water density is taken as feedback for neutronic calculation. Both co-current flow mode and counter-current flow mode were considered to model water flow scheme in peripheral and inner fuel assembly, respectively.

2.3. Equilibrium core design method

The equilibrium core design method is shown in Fig. 5. The equilibrium core, in this study, is defined such that the burnup distribution and water density distribution at the beginning of (n)th cycle(BOC) are identical to those at the beginning of $(n+1)$th cycle of operation. After all core design parameters are determined, the first cycle is calculated with neutronic and thermal-hydraulic coupling until water density distributions are converged. In order to simplify calculations, coupling calculations are performed through the cycle. Then, according to fuel reload pattern, burnup distribution of the second cycle is obtained. The core calculations for one cycle of operation, followed by the replacement of fuel assemblies, are repeated until BOC burnup distribution is converged. When BOC

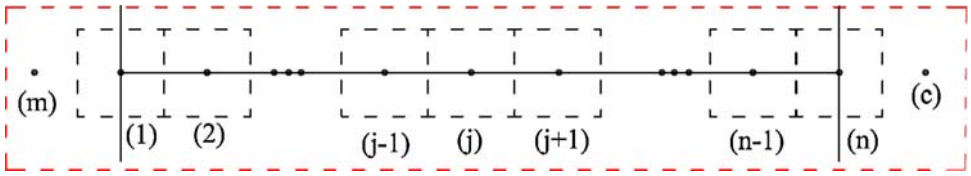

Fig. 4. Control volume division.

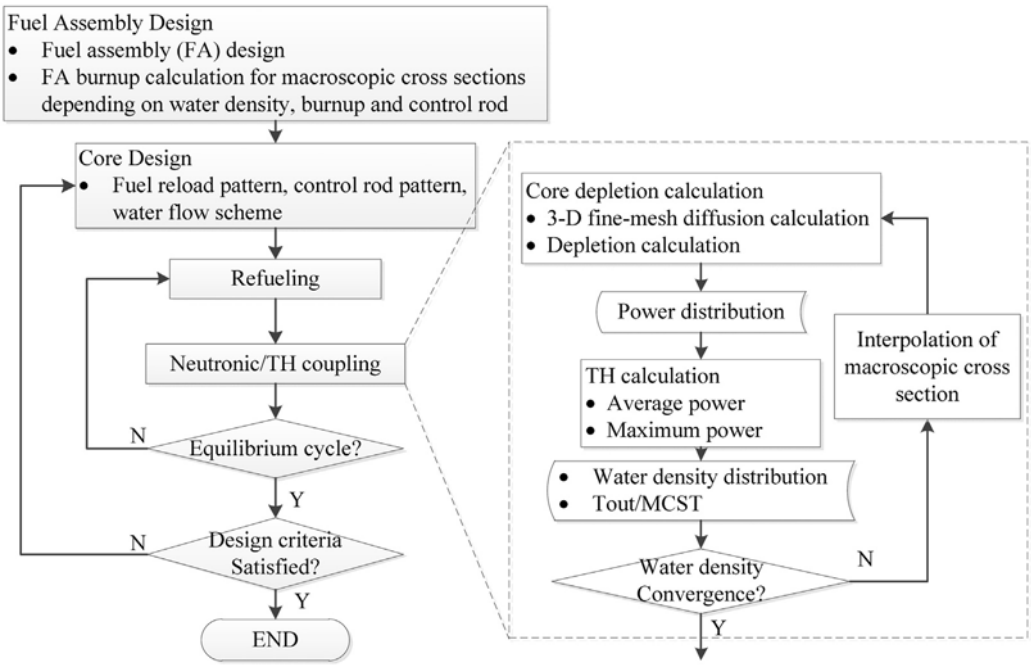

Fig. 5. Equilibrium core design method.

burnup distribution is converged, the equilibrium core is reached by definition.

3. Fuel assembly design

3.1. Fuel pin design

As shown in Fig. 6, the annular fuel pin consists of 7 rings. From inside to outside, they are moderator channel, inner cladding, thermal insulation layer, inner gap, fuel meat, outer gap, outer cladding, respectively. Moderator flows in the moderator channel and coolant flows outside of the fuel rod. In order to achieve a high coolant velocity which is beneficial for heat transfer coefficient, the hexagonal arrangement is chosen. ZrO_2 layer is used as thermal insulation to keep the moderator temperature low. The material of the cladding is SS316L following that of the previous study (Zhao et al., 2013).

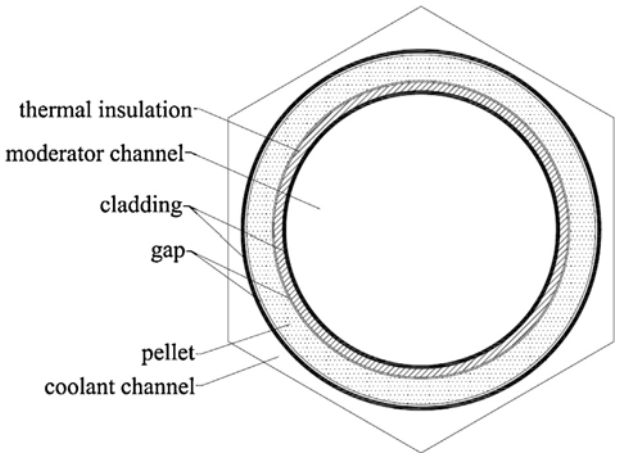

Fig. 6. Fuel pin structure.

The neutronic performance of the fuel assembly mainly depends on that of the annular fuel pin. Thus the annular fuel pin was taken as calculation model for optimization. There are several parameters of the fuel pin, i.e., the radius of the moderator channel (R1), the thickness of inner and outer cladding (Dcladding), the thickness of the thermal insulation (Dins), the width of the gap (Wgap), the thickness of the fuel meat (Dfuel), the width of space between outer cladding of two adjacent fuel rods (Dg). From the mechanical point of view, the thickness of cladding and the width of the gap were chosen to be 0.5 and 0.06 mm, respectively. The neutronic performance of the fuel pin is affected by the remaining four parameters. In order to analyze their effect and optimize the design, three variables are proposed, i.e., HU, FC, FA. HU is the nucleon density ratio of hydrogen to uranium 235. It is in proportion to the moderation. FC is the mass ratio of the fuel pellet to the cladding. It is in inversely proportion to the neutron absorption. FA is the area of the fuel pellet. It is in proportion to the fuel mass. The thickness of thermal insulation has to be greater than 2 mm to keep the moderator temperature under the pseudo critical temperature as a matter of experience. The ranges for four variables are given in Table 1. The results of 21,000 different geometry schemes are shown in Fig. 7 and the partial enlargements are shown in Fig. 8.

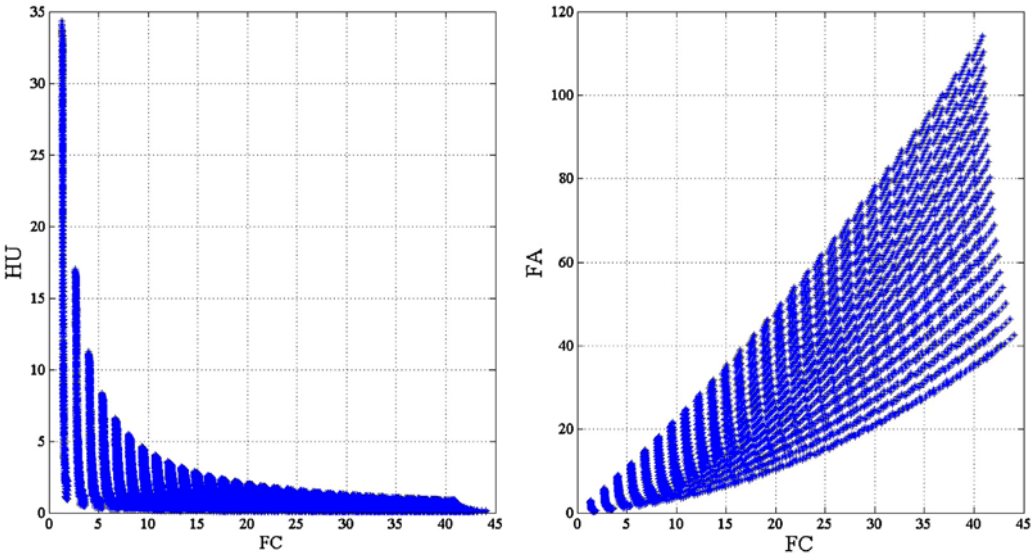

Fig. 7. Results of different schemes.

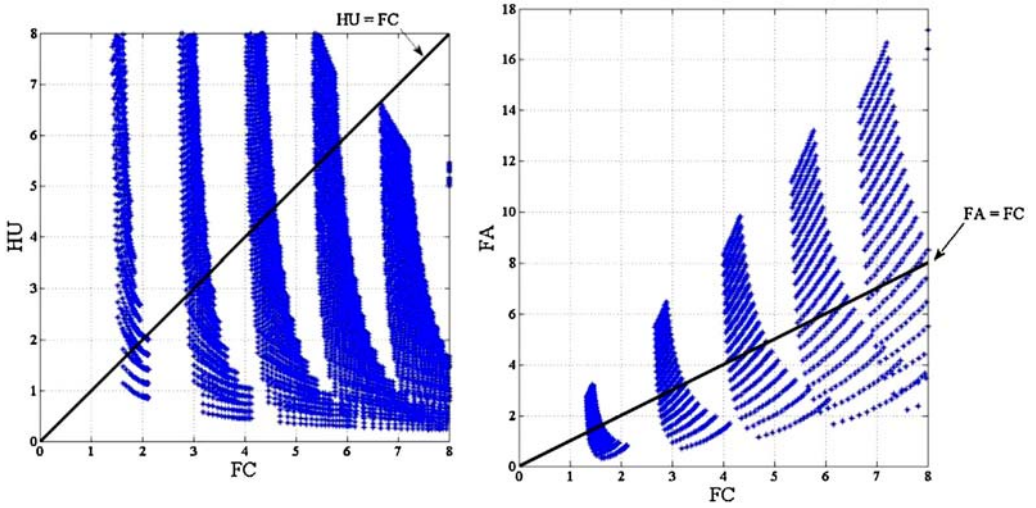

Fig. 8. Zoom in of Fig. 6.

Table 1
Ranges of parameters.

Parameter	Star	Step	End
R1 (cm)	0.2	0.2	4.0
Dins (cm)	0.2	0.05	0.5
Dfuel (cm)	0.1	0.1	3.0
Dg (cm)	0.1	0.1	0.5

From Fig. 7, some cases with different values of HU and FC are chosen and are shown in Table 2. The two-dimensional transport calculations of the fuel pin were carried out with reflective boundary. The fuel enrichment is 6 wt%. The moderator and coolant density are 0.6 and 0.15 g/cm^3, respectively. The curves of the infinite multiplication factor vs. burnup are shown in Fig. 9. The burnup of the fuel pin has to be around 40 GWd/tU to achieve high core average discharge burnup. Cases with small values of FC or HU (case 1 and case 2) are not suitable because the moderation is not enough or the neutron absorption is too high. Case 3 is better than case 4 because of more fuel load (larger FA). Case 5 keeps a balance between the moderation and the neutron absorption and achieves a better performance with less amount of fuel.

According to the above results, cases around the diagonal line need some attention. Some of these cases are listed in Table 3 and the results are shown in Fig. 10. As can be seen in Fig. 10, the fuel pin

Table 2
Typical cases.

Case	R1 (cm)	Dins (cm)	Dfuel (cm)	Dg (cm)	FA	FC	HU
1	1.9	0.96	1.0	0.1	21.463	15.181	1.042
2	1.9	0.21	0.15	0.5	2.112	2.053	10.525
3	1.9	0.41	0.45	0.3	7.326	6.376	3.01
4	1.9	0.91	0.2	0.3	3.727	3.082	6.002
5	1.9	0.06	0.35	0.1	4.818	4.63	4.309

Table 3
Cases around the diagonal line.

Case	R1 (cm)	Dins (cm)	Dfuel (cm)	Dg (cm)	FA	FC	HU
6	0.8	0.2	0.2	0.1	1.453	2.857	2.692
7	1.6	0.25	0.3	0.1	3.875	4.168	3.855
8	2.8	0.35	0.4	0.1	8.56	5.502	5.25
9	3.7	0.46	0.45	0.1	12.557	6.192	6.2171
10	1.8	0.2	0.3	0.1	4.158	4.1	4.509
11	2.0	0.25	0.3	0.1	4.629	4.124	4.986

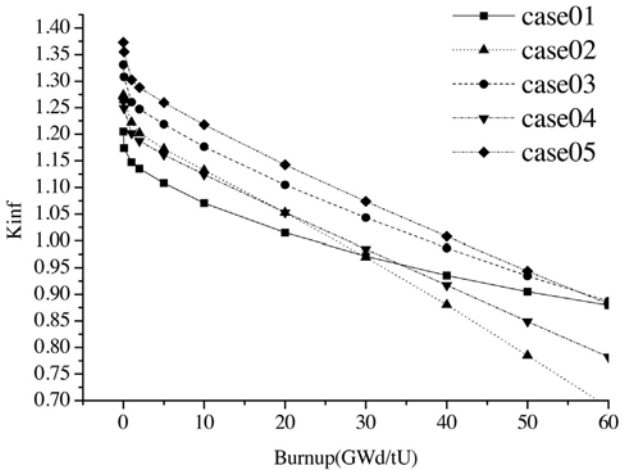

Fig. 9. *K*-infinity versus burnup for cases 01–05.

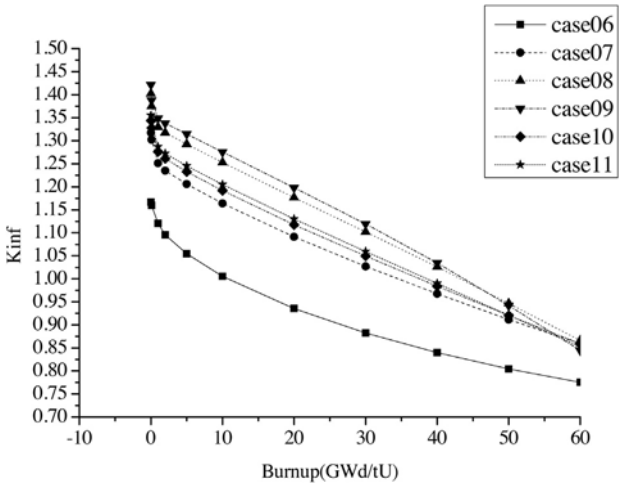

Fig. 10. *K*-infinity versus burnup for cases 06–11.

burnup increases, as the fuel load becomes larger. Note that when the fuel load is large enough (FA is around 8.0), the increase of the fuel load has less contribution on the assembly burnup. Besides, cases with large fuel load have larger initial reactivity which could cause more control rods at the beginning of the core cycle. Taking above all into account, case 11 is chosen for fuel pin design. The detail dimensions of the annular pin are shown in Table 4.

Table 4
Dimensions of annular pin.

Parameters	Values (mm)
Radius of moderator channel	20.0
Thickness of cladding	0.5
Thickness of thermal insulator	2.5
Thickness of fuel meat	3.0
Outer radius of annular pin	26.62
Annular pin pitch	54.24

3.2. Fuel assembly design

Based on the fuel pin design given in Section 3.1, the fuel assembly design was proposed. The hexagonal geometry is chosen to enhance the velocity of coolant. The fuel pin number for this geometry can be 7, 19 and 37, and the assembly pitch for the mentioned three cases are about 14, 25 and 33 cm; respectively. If smaller assembly is selected, more number of assemblies is required in the core. This will make it easier to flatten the core radial power distribution by adjusting the fuel loading pattern. But this will make the shuffling procedure more complex. Considering both factors, the number of fuel pins is determined to be 19. The horizontal cross section of a fuel assembly is shown in Fig. 11. The assembly pitch is 24.61 cm.

At the center of each pin, there is a guide tube for neutron instrumentation or control rod. The thickness of the assembly box was determined to be 2.0 mm. The material is also SS316L. In order to evaluate the local power peaking factor, the two-dimensional transport calculation of this fuel assembly was carried out at the average condition (coolant density at 0.15 g/cm^3, moderator density at 0.6 g/cm^3, fuel enrichment at 5.9 wt%). The power peaking factor (PPF) of the fuel assembly is 1.008. This is rather low because of uniform moderation for each annular pin.

In order to reduce the initial excess reactivity, burnable poison (Gd_2O_3) was mixed with the fuel. Different schemes were evaluated. The poison rod position and results are illustrated in Fig. 12 and Table 5 respectively. The target is to lower the local PPF while reducing the initial excess reactivity. Case 1 shows the result of assembly without burnable poison. As the assembly local power distribution is flat, mixing equal burnable poison with each fuel rod will keep the low PPF. However, the fuel rod is large; Even 0.1%

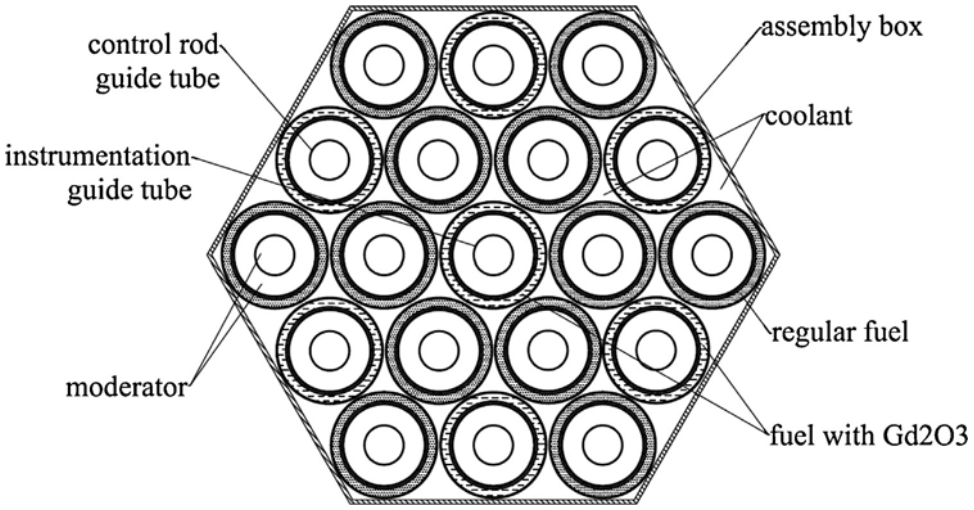

Fig. 11. Horizontal cross section of the FA.

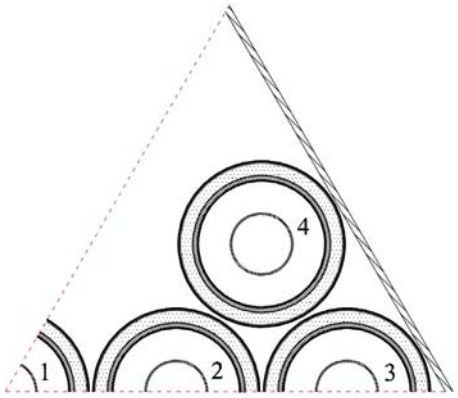

Fig. 12. Description of poison rod position (1/6th assembly).

Table 5
Candidate schemes and results.

Case	Poison position	Gd_2O_3 weight percent (%)	PPF	Initial kinf
1	None	0	1.008	1.324
2	1,2,3,4	1.0	1.01	0.533
3	1,2,3,4	0.1	1.01	0.938
4	2	1.0	1.328	0.936
5	2	0.1	1.097	1.173
6	4	0.1	1.087	1.166
7	1,2	0.1	1.15	1.157
8	1,3	0.1	1.088	1.147
9	1,4	0.1	1.071	1.141
10	1,2,4	0.1	1.16	1.032
11	1,3,4	0.1	1.126	1.033

poison can make the initial excess reactivity negative. Adding poison to fuel rod will increase the PPF, but it will decrease by reducing the poison weight percent. According to the results, case 9, which gives the lowest PPF and relatively low initial kinf, is chosen, as shown in Fig. 11.

The cluster-type control rod units (70% enriched B_4C) are inserted from the top of the core. Each control rod is a solid cylinder with a diameter of 1.7 cm. The control rod cladding (SS316L) thickness is 0.5 mm.

4. Core design

4.1. Design summary

The target core is operating at the pressure of 25 MPa. The average inlet temperature is 280 °C and the average outlet temperature is set to be above 500 °C for higher thermal efficiency. The thermal efficiency is 43.8% for the outlet temperature. Thus the thermal power is 2283 MWt for electrical power scale of 1000 MWe. The height of the core is 4.2 m. The average discharge burnup is 45 GWd/tU. The core life is 18 months (500 days). The initial fuel inventory of the core is about 75tons. The core is a three-batch core with one fourth cycle fuel assembly loaded at the center and the core is 60° symmetric, therefore, the number of fuel assemblies should be given by $18N+1$, where N is fuel number of each batch. Thus, the number of fuel assemblies is 235.

The following principles are considered to ensure fuel and core safety:

- Positive water density reactivity effect (negative void reactivity effect).
- Maximum cladding surface temperature (MCST) less than or equal to 650 °C.
- Maximum fuel temperature (MFT) less than 2520 °C.
- The core shutdown margin greater than or equal to 1.0% dk/k.

However, because of the internal and external cooling of the annular fuel, the maximum average linear heat generation was not taken as design criterion. Instead, the maximum fuel temperature was used as criterion. It should be less than the melting point of the fuel. Taking 10% safety margin into account, the limit is set to be 2520 °C.

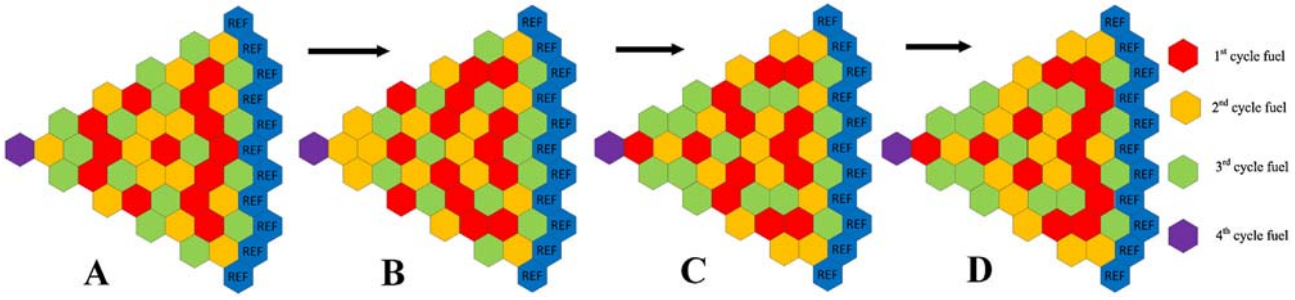

Fig. 13. Evolution of the loading pattern (1/6th core).

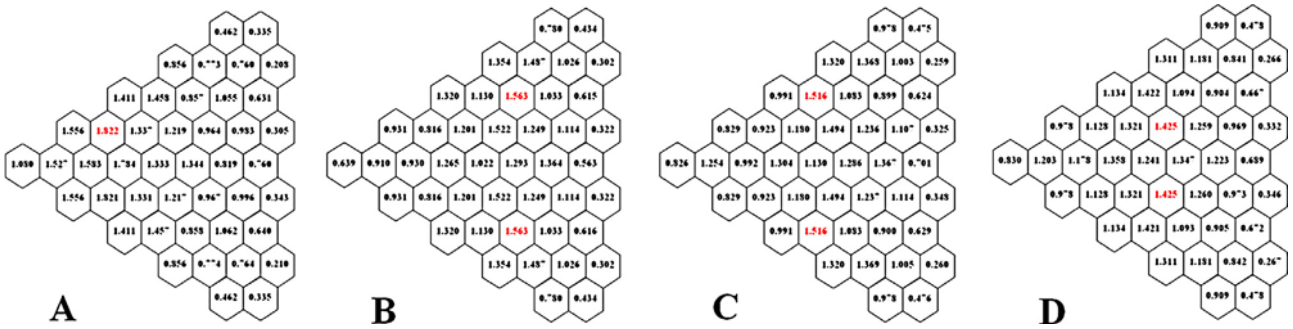

Fig. 14. Radial power distributions of loading patterns (1/6th core).

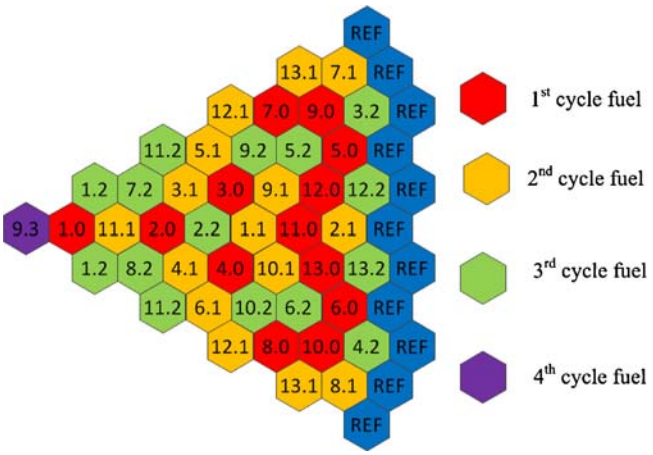

Fig. 15. Fuel loading pattern (1/6th core).

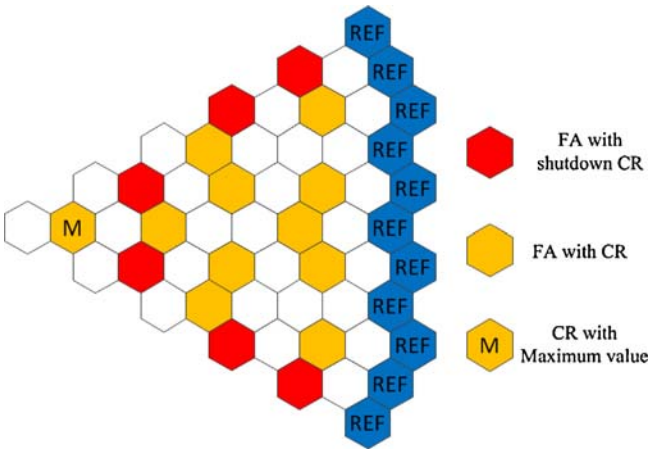

Fig. 17. Control rod pattern (1/6th core).

4.2. Fuel loading pattern

The fuel loading pattern has drastic effect on the performance of the core. It will affect the neutron leakage and power distribution. The low leakage loading pattern can decrease the required fuel enrichment. Lower cladding surface temperature can be obtained for loading pattern with more flat power distribution.

Many optimizations had been done to find a proper loading pattern. Four main designs and their results are illustrated in Fig. 13 and Fig. 14. The results in Fig. 14 are the radial power distributions at the BOC of the equilibrium core. At the EOC, the radial power distribution is more flat. In pattern A, the power peak appears in the fresh fuel assembly near the center of the core. Fresh fuel assemblies around the periphery have less power. This is because that the neutron leakage in the center is less than that at the periphery. Loading more fresh fuel assemblies in the middle area is a good way to reduce the PPF as shown in pattern B. More number of second cycle fuel assemblies is placed in the center to make up the absence of fresh fuel in this area. The radial PPF reduces as expected. For further improvements, one fresh fuel assembly is placed in the center (pattern C) and adjacent fresh fuel assemblies in the middle area are separated (pattern D). Pattern D has the lowest PPF and is taken as the loading pattern in this design.

The fuel loading pattern and shuffling scheme for one-sixth symmetric core are shown in Fig. 15. The number in each assembly indicates the shuffling scheme. Take fuel group 1 as an example, fuel assembly "1.0" is fresh, at the end of a cycle it is moved to the position of 1.1, while fuel assembly of 1.1 is moved to the position of 1.2 and fuel assembly of 1.2 is moved out of the core. Hexagon with "REF" means reflector.

4.3. Water flow scheme

Two-pass flow scheme was chosen to achieve high average coolant outlet temperature. As shown in Fig. 16, 95% of the feed water is led to upper dome and the rest flows down through the downcomer. The water in the upper dome is distributed to moderator and coolant channel, and then it flows down thought the core. All of the feed water mixes uniformly at the lower plenum and rises upward through the coolant channel of inner fuel assemblies to outlet.

4.4. Axial fuel enrichment distribution

In order to flatten axial power distribution, fuel assembly is axially divided into three partitions with different enrichments. Enrichments of top, middle and bottom parts are 5.5, 5.8 and 6.4 wt%, respectively. The heights of top, middle and bottom parts are 1.26, 1.68 and 1.26 m, respectively. The average fuel enrichment is 5.89 wt%.

4.5. Control rod pattern

The control rod loading pattern is shown in Fig. 17 for one-sixth symmetric core. Out of total 235 fuel assemblies, 66 fuel assemblies are inserted with control rods for controlling the excess

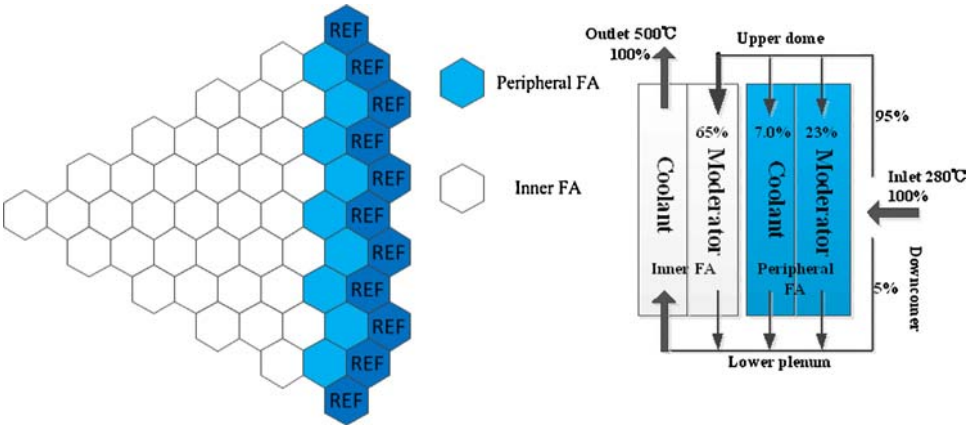

Fig. 16. Water flow scheme (1/6th core).

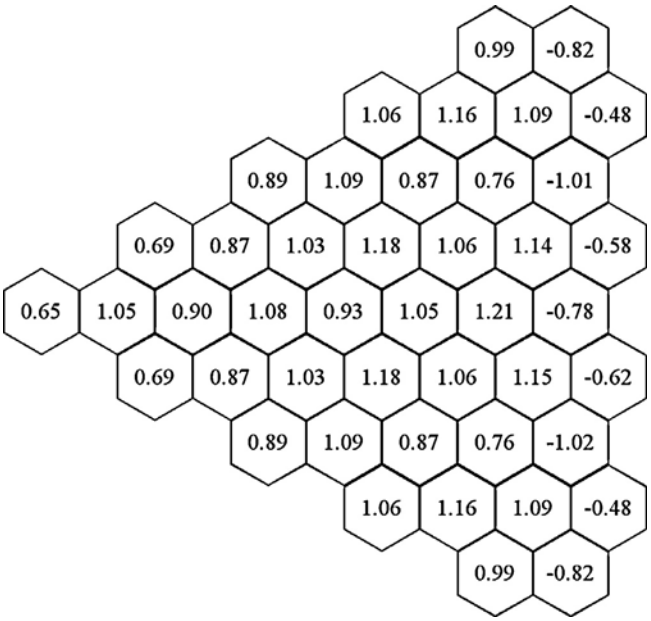

Fig. 18. Coolant flow rate distribution (1/6th core).

Table 6
Equilibrium core parameters.

Parameter	Value
Operating pressure (MPa)	25
Thermal/electrical power (MW)	2280/1000
Cycle length (EFPD)	500
No. of FA	235
Equivalent diameter/active length (m)	3.81/4.2
Average outlet temperature (°C)	500
Mass flow rate (kg/s)	1178
Fuel enrichment bottom/mid/top/average (wt%)	5.5/5.8/6.4/5.89
FA average discharge burnup (GWd/t)	47.0
Maximum discharge burnup (GWd/t)	64.0
Keff at BOC/EOC	1.116/1.008
MFT (°C)	1424
MCST (°C)	639

reactivity. Besides, 24 shutdown control rods are introduced to provide enough shutdown margins.

5. Results of equilibrium core

Primary system parameters of the equilibrium core are shown in Table 6.

5.1. Coolant flow rate distribution

The coolant flow rate distribution is shown in Fig. 18. The coolant flow rate in inner fuel assemblies is searched through the cycle to satisfy the MCST criterion. The negative numbers in peripheral

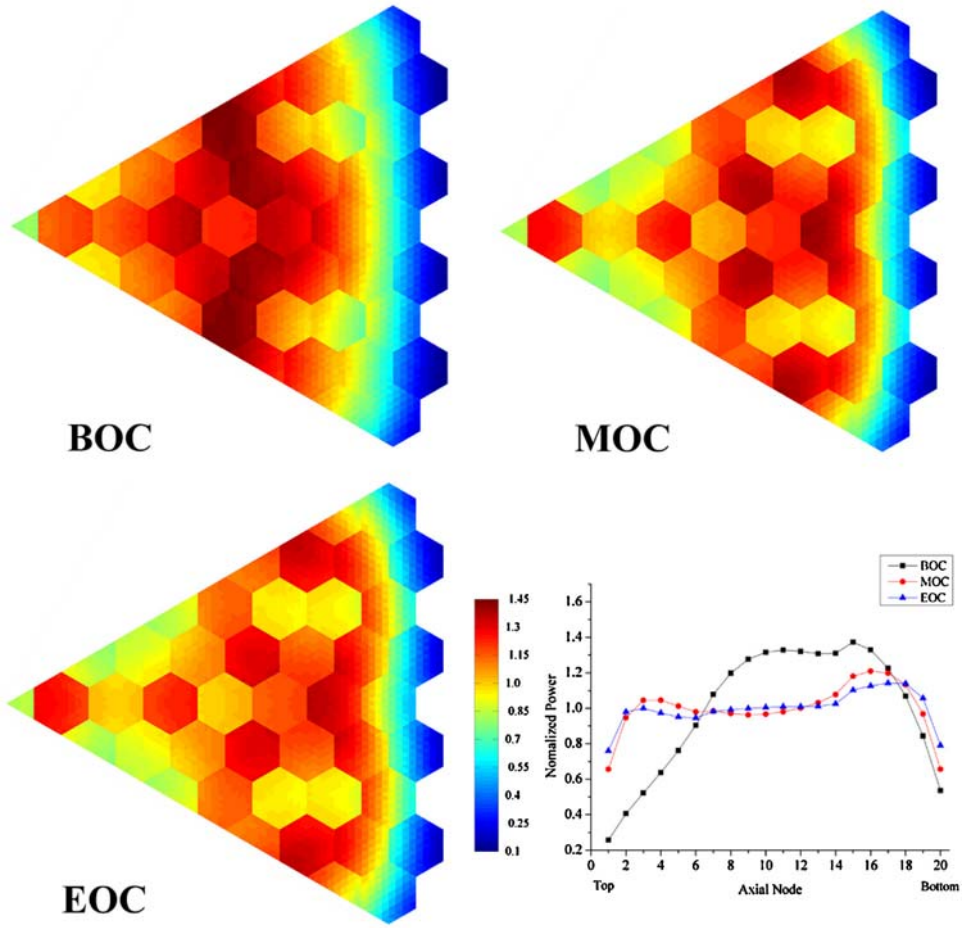

Fig. 19. Radial (1/6th core) and axial power distribution.

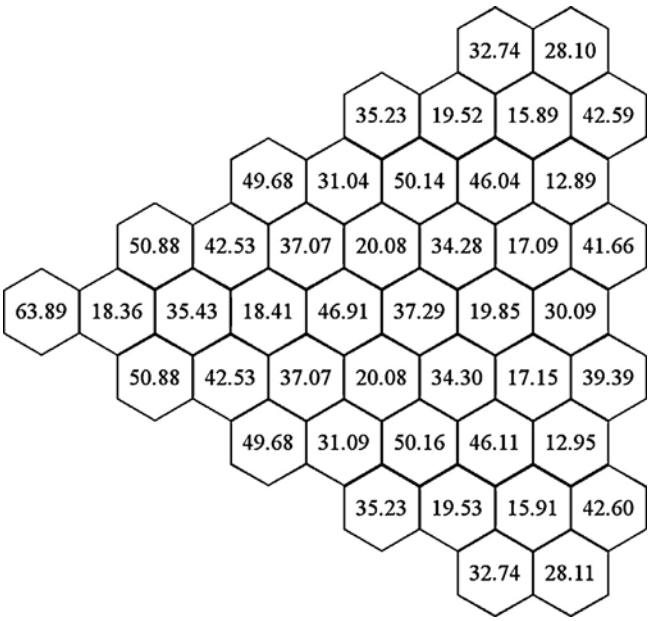

Fig. 20. Burnup distribution at the EOC (1/6th core, GWd/tU).

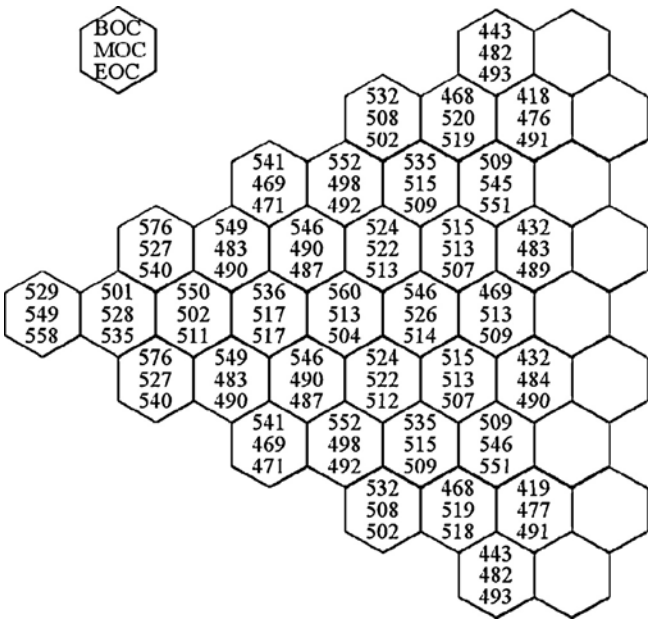

Fig. 21. Coolant outlet temperature distribution (1/6th core).

assemblies mean the coolant flows downwards. The absolute values in all assemblies denote the ratio of the coolant flow rate in this fuel assembly relative to the average flow rate of inner fuel assemblies/peripheral fuel assemblies. The moderator flow rate is the same in all assemblies.

5.2. Power distribution

Axially and horizontally averaged radial power distribution at BOC, middle of a cycle (MOC) and EOC are shown in Fig. 19. The radial power peaking factors (RPPF) is defined as the ratio of the maximum fuel assembly power to the average fuel assembly power in the core. The RPPF at BOC, MOC and EOC are 1.425, 1.375 and 1.333, respectively. The total power peaking factor (TPPF) is defined as the ratio of the maximum mesh power to the average mesh power in the core. The TPPF at BOC, MOC and EOC are 1.99, 1.71 and 1.60, respectively.

The axial PPF is kept lower than 1.4 throughout the cycle. Power peak appears at the bottom through the cycle because of relatively high enrichment. The power distribution becomes more flat as the burn-up increases and the axial PPF decreases to 1.14 at EOC.

At the end of equilibrium cycle, the axially averaged radial burnup distribution is given in Fig. 20 for 1/6th core. The maximum discharge burnup is 63.9 GWd/tU and the average burnup is 47.2 GWd/tU.

5.3. Coolant temperature, MCST, MFT distribution

The coolant outlet temperature, MCST and MFT distributions at BOC, MOC and EOC for 1/6th symmetric core are shown in Figs. 21–23. All coolant comes out through the inner fuel assemblies and the average coolant outlet temperature is 500 °C. The MCST through the cycle is 638 °C, which satisfies the design criterion. The MFT through the cycle is 1424 °C, which is much lower than the limit.

5.4. Void reactivity effect and Doppler reactivity coefficient

By increasing void fraction, void reactivity effect (in units of mk, 1 mk = 100 pcm) for a fuel assembly changes as shown in Fig. 24. It decreases as void fraction and burnup increase, and keeps negative.

The void reactivity effect for the equilibrium core is also evaluated by assuming the coolant loss. The effects at BOC and EOC are −0.42%dk/k and −1.01%dk/k, respectively. It is also calculated by assuming the feed water loss. The effects at BOC and EOC are −32.3%dk/k and −29.0%dk/k, respectively. The design criterion of negative void reactivity effects is satisfied.

The Doppler reactivity coefficient was calculated for a typical fuel assembly. The coefficients at 0 and 45 GWd/tU are −1.981E-05 and −2.227E-05, respectively.

In the evaluation of cold shutdown margin, the water density was assumed to be 1.0 g/cm^3, all fuel and structural material temperature are chosen as 300 K. The calculation was carried out at cycle burnup 0.0GWd/t for the whole core. The cluster type control rods except the maximum worth control rod (see Fig. 17) were inserted completely. The cold shutdown margin is 2.0%dk/k.

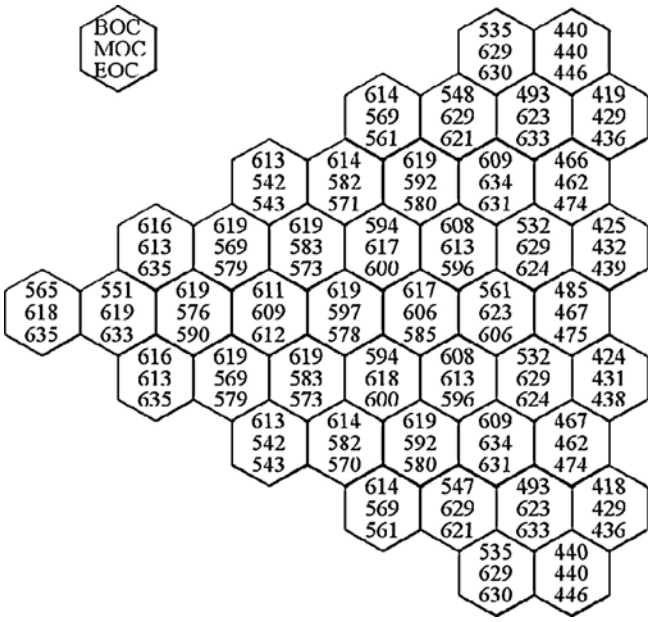

Fig. 22. MCST distribution (1/6th core)

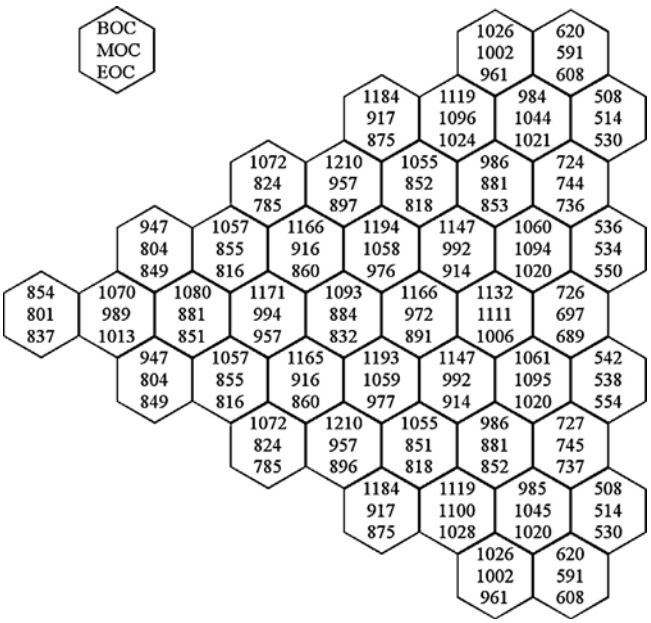

Fig. 23. MFT distribution (1/6th core).

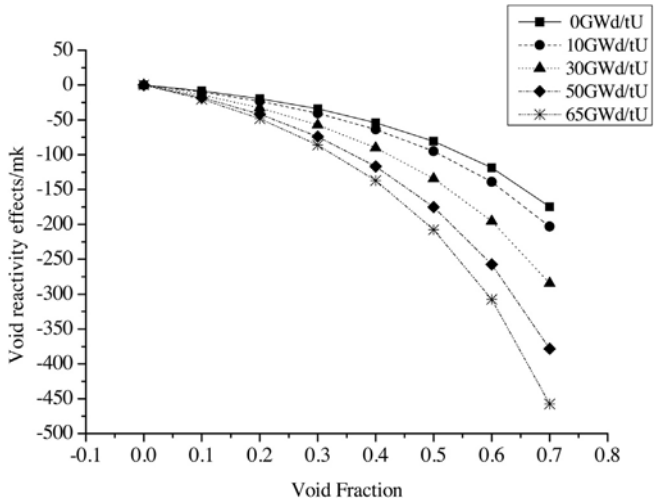

Fig. 24. Void reactivity effect.

6. Conclusions

Annular fuel with both internal and external cooling was proposed in this study to reduce the cladding and fuel temperature. Besides, the center moderator channel brings uniform local power distribution. Some research was carried out to find better fuel pin design. During the optimization, three variables were proposed to evaluate neutron moderation, neutron absorption and fuel load for each case. According to the analysis, the cases that keep balance among these variables have better neutron performance. In the fuel assembly, some pins are mixed with burnable poison. The content of burnable poison in each pin cannot be high because the fuel pin is large and high poison content can cause negative initial reactivity. In addition, the effect on local power peaking factor can be decreased by decreasing the amount of burnable poison.

Based on this assembly design, the low leakage loading pattern was used and optimized to achieve more uniform power distribution. The assembly enrichment was divided into three partitions for the same purpose. The two-pass flow scheme was used to increase the outlet temperature. With these designs, an equilibrium core was searched using neutronics and thermal-hydraulic coupling calculation. The results show that the equilibrium core has satisfied all the objectives and design criteria. The fuel temperature is much lower than the design criteria.

Another advantage of the annular fuel is its high power density. In this study, the power density is relatively low to minimize the fuel enrichment. By increasing the fuel enrichment, the power density can be increased to decrease the cost. This can be carried out in the future.

Acknowledgments

This work is financially supported by the National Science Foundation of China (approved number 91126005 and 11105104).

References

Ellis, T.S., 2006. Advanced design concepts for PWR and BWR high-performance annular fuel assemblies. M.S. thesis, Massachusetts Institute of Technology, http://dspace.mit.edu/handle/1721.1/41268

Feng, D.D., 2006. Innovative fuel designs for high power density pressurized water reactor. Ph.D. thesis, Massachusetts Institute of Technology, http://hdl.handle.net/1721.1/41283

Fowler, T.B., Vondy, D.R., Cunningham, G.W., 1971. Nuclear Reactor Core Analysis code CITATION, ORNL-TM-2496. Oak Ridge National Laboratory.

Kamei, K., Yamaji, A., Ishiwatari, Y., et al., 2006. Fuel and core design of super light water reactor with low leakage fuel loading pattern. Journal of Nuclear Science and Technology 43, 129–139.

Liu, X.J., Cheng, X., 2009. Thermal-hydraulic and neutron-physical characteristics of a new SCWR fuel assembly. Journal of Annals of Nuclear Energy 36, 28–36.

Liu, X.J., Cheng, X., 2010. Core and sub-channel analysis of SCWR with mixed spectrum core. Journal of Annals of Nuclear Energy 37, 1674–1682.

Maráczy, C., Hegyi, G., Hordósy, G., et al., 2011. HPLWR equilibrium core design with the KARATE-code system. Journal of Progress in Nuclear Energy 53, 267–277.

Marleau, G., Hébert, A., Roy, R., 2000. A user's guide for DRAGON. In: Report IGE-174 Rev. 5. École Polytechnique de Montréal.

Paolo, M., 2005. Design of annular fuel for high power density BWRs. M.S. thesis, Massachusetts Institute of Technology, http://hdl.handle.net/1721.1/34448

Schulenberg, T., Maráczy, C., et al., 2011. Assessment of the HPLWR thermal core design. In: ISSCWR-5, Vancouver, Canada, March, pp. 13–16.

Spang, B., 2010. Thermodynamic and Transport Properties of Water and Steam, http://www.cheresources.com/content/articles/physical-properties/thermodynamic-and-transport-properties-of-water-and-steam

Watts, M.J., Chou, C.T., 1982. Mixed convection heat transfer to supercritical pressure water. In: Proceedings of 7th International Heat Transfer Conference, vol. 3, Munchen, Germany, pp. 495–500.

Yamaji, A., Kamei, K., Oka, Y., et al., 2005a. Improved core design of the high temperature supercritical-pressure light water reactor. Journal of Annals of Nuclear Energy 32, 651–670.

Yamaji, A., Oka, Y., Koshizuka, S., 2005b. Three-dimensional core design of high temperature supercritical-pressure light water reactor with neutronic and thermal-hydraulic coupling. Journal of Nuclear Science and Technology 42, 8–19.

Yang, P., Cao, L.Z., Wu, H.C., et al., 2011. Core design study on CANDU-SCWR with 3D neutronics/thermal-hydraulics coupling. Journal of Nuclear Engineering and Design 241, 4714–4719.

Zhao, C.Q., Cao, L.Z., Wu, H.C., et al., 2013. Conceptual design of a supercritical water reactor with double-row-rod assembly. Journal of Progress in Nuclear Energy 63, 86–95.